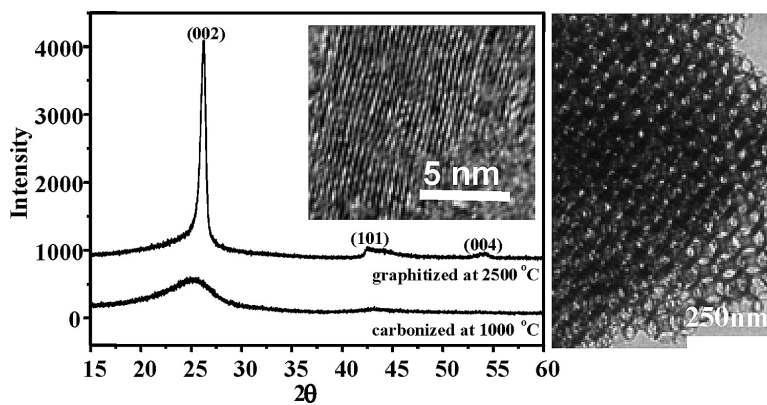


## Graphitized Pitch-Based Carbons with Ordered Nanopores Synthesized by Using Colloidal Crystals as Templates

Suk Bon Yoon, Geun Seok Chai, Soon Ki Kang, Jong-Sung Yu, Kamil P. Gierszal, and Mietek Jaroniec

*J. Am. Chem. Soc.*, **2005**, 127 (12), 4188-4189 • DOI: 10.1021/ja0423466 • Publication Date (Web): 08 March 2005

Downloaded from <http://pubs.acs.org> on March 24, 2009



### More About This Article

Additional resources and features associated with this article are available within the HTML version:

- Supporting Information
- Links to the 21 articles that cite this article, as of the time of this article download
- Access to high resolution figures
- Links to articles and content related to this article
- Copyright permission to reproduce figures and/or text from this article

[View the Full Text HTML](#)

## Graphitized Pitch-Based Carbons with Ordered Nanopores Synthesized by Using Colloidal Crystals as Templates

Suk Bon Yoon,<sup>†</sup> Geun Seok Chai,<sup>†</sup> Soon Ki Kang,<sup>†</sup> Jong-Sung Yu,<sup>\*,†</sup> Kamil P. Gierszal,<sup>‡</sup> and Mietek Jaroniec<sup>\*,‡</sup>

*Department of Chemistry, Hannam University, Daejeon, 306-791 Korea, and Department of Chemistry, Kent State University, Kent, Ohio 44242*

Received December 20, 2004; E-mail: jsyu@hannam.ac.kr; jaroniec@kent.edu

Nanostructured carbon materials have attracted tremendous attention for their possible applications as adsorbents, catalyst supports, nanocomposites, electrode materials, and storage media. Recently, significant progress has been made in the synthesis of ordered nanoporous carbons (ONCs) by using zeolites,<sup>1</sup> ordered mesoporous silicas (OMS),<sup>2</sup> and colloidal crystals<sup>3</sup> as solid templates. Sucrose, phenolic resin, furfuryl alcohol, polydivinylbenzene, and polyacrylonitrile are usually used as carbon precursors. The resulting carbons are usually amorphous because carbonization was carried out at a temperature between 700 and 1000 °C, and no graphitization (heating in argon at a temperature between 2000 and 3000 °C) was performed.<sup>1–3</sup> The use of carbon precursors that contain graphitic building blocks (e.g., pitch, acenaphthene) afforded carbons with some degree of graphitization even without additional graphitization.<sup>4</sup> However, carbonization of these precursors without further graphitization is not sufficient to obtain highly graphitized carbons. There are a few reports on porous graphitized carbons, which were obtained by heating under argon at a temperature exceeding 2000 °C.<sup>5,6</sup> Li et al.<sup>5</sup> reported synthesis of pitch-based graphitized carbon with uniform spherical mesopores created by using silica colloids as template. Fuertes et al.<sup>6</sup> carbonized the OMS–poly(vinyl chloride) nanocomposites, which after template dissolution were graphitized. Although the resulting graphitized carbons were mesoporous, their structural ordering was rather poor. To the best of our knowledge, highly graphitized ONC has not yet been reported.

Here we propose a simple method for the preparation of highly graphitized ONCs by using commercial mesophase pitch as carbon precursor and siliceous colloidal crystal as template. The mesophase pitch is an attractive carbon precursor because it is a mixture of polyaromatic hydrocarbons capable of forming, during carbonization, quite large graphite domains, which are significantly enlarged during the graphitization process. Since silica colloids of different sizes (above 6 nm) and narrow particle size distribution are commercially available, the pore size tailoring in the resulting ONCs is not a difficult task. Although colloidal crystals of large silica spheres (150–300 nm in diameter) have been coated with “graphite” by chemical vapor deposition, this process was carried out at relatively low temperature (750–850 °C) and afforded 3D ordered macroporous carbons only.<sup>3a</sup> The current work shows an attractive way to prepare graphitized ONCs with pores on the borderline between mesopores and macropores, that is, 40–100 nm.

The synthesis of the graphitized ONCs was carried out by incorporation of mesophase pitch dissolved in quinoline under static vacuum into the void space of the silica colloidal crystal (colloid’s size about 69 nm), its stabilization at 180–330 °C with heating

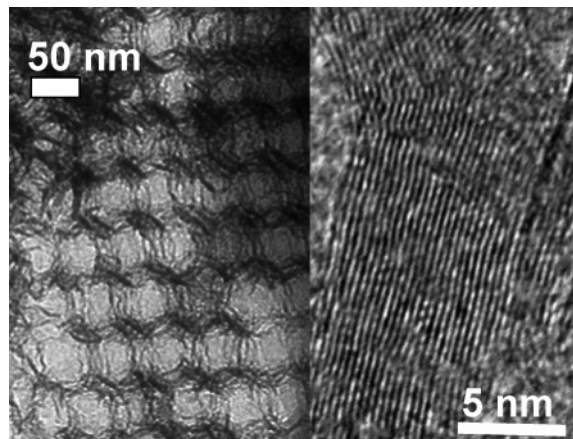


**Figure 1.** TEM images of ONC graphitized under argon at 2500 °C.

rate of 1 °C/min and carbonization at 1000 °C for 7 h with heating rate of 5 °C/min followed by removal of the silica template with diluted HF solution. The resulting carbon was washed with distilled water and dried under air at 50 °C. Some amount of this carbon was further heated at high temperature (2500 °C for 30 min) in argon atmosphere to achieve a high graphitization degree of the carbon matrix.

Figure 1 shows TEM images at different resolution levels for the pitch-based ONC graphitized at 2500 °C. Analogous TEM images are displayed in the Supporting Information Figure 1S for the same carbon before graphitization process. While the left panels in Figure 1 and 1S show the presence of interconnected ordered spherical pores created by dissolution of colloidal crystal template, the right panels in these figures present high-resolution TEM images of pore walls. These images show a rather random stacking of graphene layers in the carbon matrix, indicating that the carbonization of mesophase pitch at 1000 °C did not give high graphitic crystallinity (see right panel in Supporting Information Figure 1S), while its subsequent graphitization led to the formation of relatively large graphite crystallinities in the carbonaceous pore walls having interlayer spacing of ~0.33 nm (see Figures 1 and 2S). The thickness of graphite domains estimated by the Scherrer equation from XRD data is about 6.3 nm.<sup>7</sup>

Shown in Figure 2 are the XRD patterns for the sample carbonized at 1000 °C and the same sample subjected to additional graphitization at 2500 °C. While the former carbon sample shows a weak broad (002) signal, which is often related to the turbostratic carbon structure having randomly oriented graphene layers, the graphitized carbon sample shows a high-intensity sharp (002) signal corresponding to the 0.34-nm-interlayer spacing along with clearly observable other (100), (101), and (004) reflections characteristic for 2D and 3D graphitic structures.

<sup>†</sup> Hannam University.  
<sup>‡</sup> Kent State University.

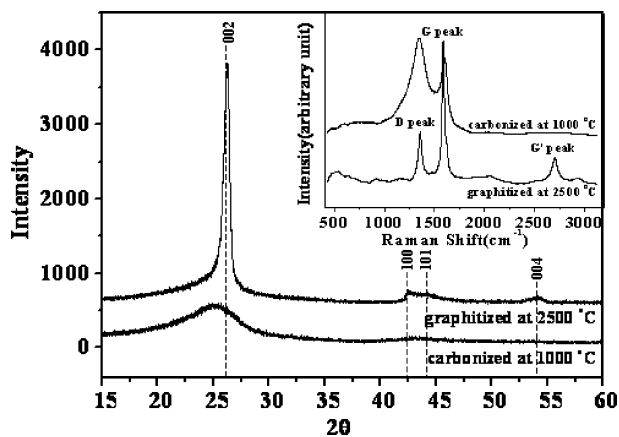


**Figure 2.** XRD patterns and Raman spectra (inset) for the pitch-based ONC studied.

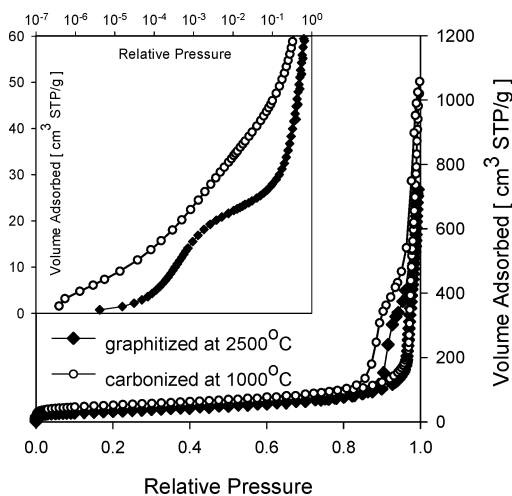


**Figure 3.** Nitrogen adsorption isotherms at  $-196\text{ }^{\circ}\text{C}$  for the pitch-based ONC samples; inset shows low-pressure adsorption isotherms plotted on a semilogarithmic scale.

Additional confirmation for high degree graphitization in the carbon sample heated at  $2500\text{ }^{\circ}\text{C}$  in argon is provided in Figure 2 (see inset), which shows Raman spectra. Graphite single crystals exhibit a high-intensity sharp G-band at  $1575\text{ cm}^{-1}$ .<sup>8</sup> An additional D-band at  $1355\text{ cm}^{-1}$  appears for carbon materials such as activated charcoal, carbon black, and vitreous carbon. The relative intensities of these two lines depend on the type of graphitic materials and reflect the degree of graphitization. As can be seen in this inset, the carbonized pitch sample shows a lower-intensity G-band signal at  $1601\text{ cm}^{-1}$  and a higher-intensity broad D-band at  $1346\text{ cm}^{-1}$ , while the graphitized sample exhibits a strong G-band signal at  $1588\text{ cm}^{-1}$  and a lower-intensity D-band at  $1356\text{ cm}^{-1}$ . The observed difference in the Raman spectra for both carbons indicates a graphitic nature of the carbon heated at  $2500\text{ }^{\circ}\text{C}$ , which is in accordance with high-resolution TEM and wide-angle XRD studies.

Shown in Figure 3 are nitrogen adsorption isotherms for the ONC samples studied. These isotherms are type IV with an H1 loop according to the IUPAC classification.<sup>9</sup> The corresponding pore size distributions obtained by the modified BJH method<sup>10</sup> are presented in Supporting Information Figure 3S. Graphitization at  $2500\text{ }^{\circ}\text{C}$  of the carbonized sample reduces the BET surface area from  $185$  to  $115\text{ m}^2/\text{g}$ . Similarly, the total pore volume is reduced from  $1.63$  to  $1.12\text{ cm}^3/\text{g}$ . However, graphitization did not change the shape of adsorption isotherm. A slight shift of the adsorption branch toward lower relative pressures is related to the structural shrinkage of the carbon during graphitization, which causes a small

decrease in the pore size from  $\sim 74$  to  $\sim 65\text{ nm}$  (see Figure 3S). Meanwhile, a small desorption branch shift toward high relative pressures reflects some increase in the opening (interconnection) between spherical pores during graphitization. A similar behavior was reported for graphitization of colloid-imprinted carbons having randomly interconnected spherical pores.<sup>5</sup> In addition, graphitization eliminates high-energy sites on the carbon surface by increasing its surface homogeneity, which is manifested by lowering nitrogen uptake at low relative pressures (see inset in Figure 3). In contrast to the carbonized sample, the nitrogen adsorption isotherm for the graphitized carbon exhibits an apparent step at the relative pressure range between  $10^{-4}$  and  $10^{-3}$  that reflects monolayer formation characteristic for highly graphitized carbons.<sup>11</sup>

A highly graphitized ONC with spherical pores on the borderline between mesopores and macropores was prepared for the first time by graphitization at  $2500\text{ }^{\circ}\text{C}$  of the pitch-based carbon obtained by using silica colloidal crystal as template. Since both silica colloids of different sizes and mesophase pitch are commercially available, the proposed method is feasible for the synthesis of larger amounts of highly graphitized ONC materials with high surface area and tailored pore widths for versatile applications.

**Acknowledgment.** J.-S. Yu thanks KOSEF (R02-2004-000-10152-0) for the financial support and KBSI at Jeonju and Deajeon for SEM and TEM measurements. The Ohio Research Challenge Grant is acknowledged (M.J.).

**Supporting Information Available:** Figures of TEM images and pore size distributions. This material is available free of charge via the Internet at <http://pubs.acs.org>.

## References

- (1) (a) Kyotani, T.; Ma, Z.; Tomita, A. *Carbon* **2003**, *41*, 1451. (b) Johnson, S. A.; Brigham, E. S.; Ollivier, P. J.; Mallouk, T. E. *Chem. Mater.* **1997**, *9*, 2448.
- (2) (a) Ryoo, R.; Joo, S. H.; Jun, S. J. *Phys. Chem. B* **1999**, *103*, 7743. (b) Lee, J.; Yoon, S.; Hyeon, T.; Oh, S. M.; Kim, K. B. *Chem. Commun.* **1999**, 2177. (c) Jun, S.; Joo, S. H.; Ryoo, R.; Kruk, M.; Jaroniec, M.; Liu, Z.; Ohsuna, T.; Terasaki, O. *J. Am. Chem. Soc.* **2000**, *122*, 10712. (d) Joo, S. H.; Choi, S. J.; Oh, I.; Kwak, J.; Liu, Z.; Terasaki, O.; Ryoo, R. *Nature* **2001**, *412*, 169. (e) Ryoo, R.; Joo, S. H.; Kruk, M.; Jaroniec, M. *Adv. Mater.* **2001**, *13*, 677. (f) Yoon, S. B.; Kim, J. Y.; Yu, J.-S. *Chem. Commun.* **2001**, 559; **2002**, 1536. (g) Vix-Cuterl, C.; Boulard, S.; Parmentier, J.; Werckmann, J.; Patarin, J. *Chem. Lett.* **2002**, 1062. (h) Yang, H.; Shi, Q.; Liu, X.; Xie, S.; Jiang, D.; Zhang, F.; Yu, C.; Tu, B.; Zhao, D. *Chem. Commun.* **2002**, 2842. (i) Lu, A.; Kiefer, A.; Schmidt, W.; Schuth, F. *Chem. Mater.* **2004**, *16*, 100. (j) Li, Z.; Del Cul, G. D.; Yan, W.; Liang, C.; Dai, S. *J. Am. Chem. Soc.* **2004**, *126*, 12782.
- (3) (a) Zakhidov, A. A.; Baughman, R. H.; Iqbal, Z.; Cui, C.; Khayrullin, I.; Dantas, S. O.; Marti, J.; Ralchenko, V. G. *Science* **1998**, *282*, 897. (b) Yu, J. S.; Yoon, S. B.; Chai, G. S. *Carbon* **2001**, *39*, 1442. (c) Yu, J.-S.; Kang, S.; Yoon, S. B.; Chai, G. S. *J. Am. Chem. Soc.* **2002**, *124*, 9382. (d) Kang, S.; Yu, J.-S.; Kruk, M.; Jaroniec, M. *Chem. Commun.* **2002**, 1670. (e) Lei, Z.; Zhang, Y.; Wang, H.; Ke, Y.; Li, J.; Li, F.; Xing, J. *J. Mater. Chem.* **2001**, *11*, 1975.
- (4) (a) Li, Z.; Jaroniec, M. *J. Am. Chem. Soc.* **2001**, *123*, 9208. (b) Jian, K.; Shim, H.-S.; Schwartzman, A.; Crawford, G. P.; Hurt, R. H. *Adv. Mater.* **2003**, *15*, 164. (c) Kim, T.-W.; Park, I.-S.; Ryoo, R. *Angew. Chem., Int. Ed.* **2003**, *42*, 4375. (d) Yang, H.; Yan, Y.; Liu, Y.; Zhang, F.; Zhang, R.; Meng, Y.; Li, M.; Xie, S.; Tu, B.; Zhao, D. *J. Phys. Chem. B* **2004**, *108*, 17320. (e) Xia, Y. D.; Mokaya, R. *Adv. Mater.* **2004**, *16*, 1553.
- (5) Li, Z.; Jaroniec, M.; Lee, Y. J.; Radovic, L. R. *Chem. Commun.* **2002**, 1346.
- (6) Fuertes, A. B.; Alvarez, S. *Carbon* **2004**, *42*, 3049.
- (7) Knox, J. H.; Kaur, B.; Millward, G. R. *J. Chromatogr.* **1986**, *352*, 3.
- (8) Cullity, B. D. *Elements of X-ray Diffraction*; Addison-Wesley: New York, 1984; Chapter 9.
- (9) Rouquerol, J.; Avnir, D.; Fairbridge, C. W.; Everett, D. H.; Haynes, J. H.; Pernicone, N.; Ramsay, J. D. F.; Sing, K. S. W.; Unger, K. K. *Pure Appl. Chem.* **1994**, *66*, 1739.
- (10) Kruk, M.; Jaroniec, M.; Sayari, A. *Langmuir* **1997**, *13*, 1435.
- (11) Kruk, M.; Li, Z.; Jaroniec, M.; Betz, W. R. *Langmuir* **1999**, *13*, 66267.

JA0423466